JOURNAL OF BACTERIOLOGY, June 1969, p. 1320-1327
Vol. 98, No. 3

Changes in the Plasma Membrane of *Escherichia coli* During Magnesium Starvation

ANNELISE FIIL[1] AND DANIEL BRANTON
Department of Botany, University of California, Berkeley, California 94720

Received for publication 10 March 1969

The effect of Mg^{++} starvation on the structure of the *Escherichia coli* cell membrane was studied with the freeze-etch technique. Special attention was paid to changes within the plane of the membrane, which in normal exponentially growing cells has a netlike arrangement of particles 2 to 6 nm in diameter. During Mg^{++} starvation, a paracrystalline particle pattern appeared on the plasma membrane, and large areas devoid of particles were seen. Although these changes are reproducibly associated with Mg^{++} starvation of the bacteria, no decrease in the Mg^{++} content of the cell envelope per se was detected, even after 24 hr of Mg^{++} deprivation. The structural changes caused by Mg^{++} deprivation appeared to involve specific and permanent alterations in membrane development. The absence of other nutrients or divalent cations did not induce similar alterations.

Magnesium deficiency in the gram-negative bacterium *Escherichia coli* has been reported to cause formation of filaments and changes in the permeability of the cell membrane (5). Electron microscopy of thin sections of *E. coli* strain B has shown that, during prolonged Mg^{++} starvation, the plasma membrane proliferates and infolds near the ends of the cell (9, 16). The infolded membranes may exhibit regularly spaced, lamellar structures with a repeat distance of 10 nm (16). However, it is not apparent how these infoldings are related to observed permeability changes (5), which one would expect to be caused by more restricted structural changes within the plane of the plasma membrane.

Because standard thin-sectioning techniques are not particularly well suited to the study of structural heterogeneity in bacterial membranes, we have examined the effects of Mg^{++} starvation in *E. coli* by the freeze-etch technique (18, 25). This method produces a three-dimensional replica of chemically untreated cells and provides clear evidence of structural changes in the plane of the bacterial cell membrane during Mg^{++} starvation.

MATERIALS AND METHODS

Organism and culture methods. The strain used, *E. coli* B/r/1, was obtained from D. J. Clark and was grown at 37 C in a glucose-supplemented mineral medium (7). For the starvation studies, $MgCl_2$ was replaced by NaCl, and the medium was further purified by allowing a culture of B/r/1 to use up any contaminant Mg^{++}. This Mg^{++}-free medium was resterilized by passage through a membrane filter (Millipore Corp., Bedford, Mass.), and extra glucose was added. A culture growing exponentially in medium with $MgCl_2$ was filtered; the bacteria were washed three times with prewarmed Mg^{++}-free medium and were resuspended in the Mg^{++}-free medium at 37 C. Control experiments with similarly prepared and preutilized media, but with Mg^{++} subsequently added, supported normal *E. coli* growth.

Freeze-etching. Exponentially growing cells and cells deprived of Mg^{++} for various lengths of time were chilled in an ice bath, centrifuged, and resuspended in the same volume of medium with 20% glycerol. After 3 hr at 4 C to reverse the slight plasmolysis that may arise initially on transfer to glycerol, the bacteria were centrifuged, and small samples of the pellet were frozen in Freon-22, cooled by liquid nitrogen. The cells were freeze-etched and the replica was cleaned, following the procedure of Moor and Mühlethaler (17). Except for Fig. 2, etching time was 2 min at −100 C. The replica was picked up on an uncovered grid and examined in a Siemens Elmiskop I. In all micrographs, shadows appear white and shadow direction is given by the encircled arrow.

Control cells frozen in their growth media without added glycerol showed the same salient structures described here for glycerol-treated cells; however, they were distorted by ice crystal growth and therefore difficult to use for illustrative purposes.

Isolation of cell envelopes and Mg^{++} determination. Bacteria were centrifuged in the cold, resuspended in deionized water at 0 C, and sonically disrupted with a Biosonik II ultrasonic probe for two 90-sec periods separated by 5 min of cooling. The wall plus membrane fraction was isolated by centrifugation (13,000 × *g*, 15 min at 6 C) through a linear sucrose gradient

[1] Present address: Department of Molecular Biology, University of Oregon, Eugene, Ore. 97403.

in D_2O with density from 1.09 to 1.25 (24). The unbroken bacteria sedimented to the bottom, whereas the envelopes were found in two bands. The slower moving band contained small wall fragments, and the faster moving band contained envelopes corresponding to half a bacterium. Electron microscopy of negatively stained material from the latter band showed that the plasma membrane was contained inside the cell wall. Both bands were washed separately six times by centrifugation at 4 C with deionized water.

To determine the Mg^{++} content, both whole cells and the purified envelope fractions were wet-ashed with sulfuric acid and hydrogen peroxide. After appropriate dilution, the Mg^{++} content was measured in a double-beam atomic absorption spectrophotometer and was expressed per unit dry weight of material. Limited sample size made it difficult to determine dry weight of the envelope fractions gravimetrically. The culture medium was therefore supplemented with ^{14}C-glucose (uniformly labeled, 2 mg/ml, 0.01 μc/ml), and the ratio of ^{14}C counts to dry weight was established with whole cells. This was done by bringing 1-ml samples of whole cells to 5% with trichloroacetic acid, waiting 30 min, collecting on membrane filters, drying, weighing, and counting in a scintillation spectrometer. The dry weight of the material in similarly collected 0.1-ml samples of envelope fractions was estimated, with the whole-cell ^{14}C count to dry weight ratio.

RESULTS

Normal and Mg^{++}-depleted growth. Figure 1 shows the typical growth history of a culture such as those sampled for electron microscopy and illustrated in Fig. 2 to 12. After transfer to Mg^{++}-free medium, growth stopped within 3 hr after about a 100% increase in optical density (OD) at 450 nm. OD remained constant during continued starvation up to 24 hr. The cells became 10% smaller in diameter during the first hours of starvation, as measured on a Coulter counter modified to analyze the impulses in a 512-channel pulse-height analyzer (D. A. Glaser). No filament formation was observed. Plate counting indicated that viability remained constant for 12 hr. After 24 hr of Mg^{++} starvation, only 2% of the cells retained colony-forming ability.

Exponentially growing cells. Frozen-etched *E. coli* cells did not have the wrinkled walls seen after fixation for thin-section microscopy. The only structures seen on the strain B/r/1 surface were globules ranging in size from 13 to 35 nm in diameter (Fig. 2). These globules were especially numerous over the constriction line in dividing cells, but were also seen in the suspending medium. They may correspond to the mucopeptide-free vesicles of outer wall material found by de Petris (21) in thin sections. Remsen (22) noted similar globules in *Bacillus subtilis*.

The fracture process used in freeze-etching

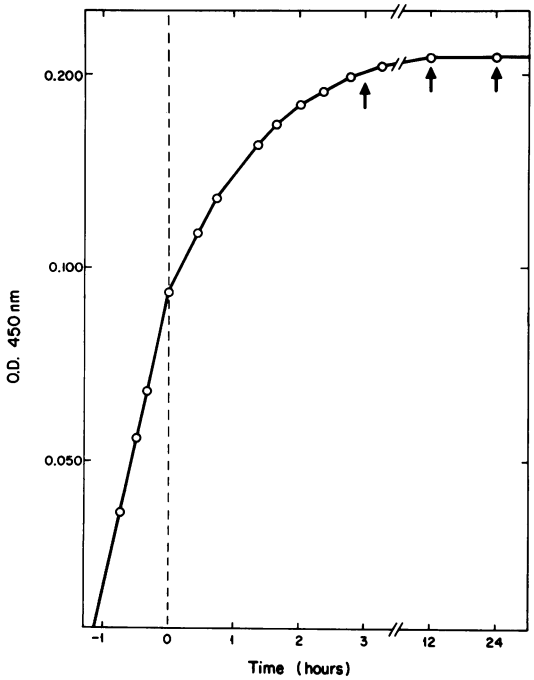

FIG. 1. *E. coli B/r/1 growing exponentially in minimal medium with $MgCl_2$ was transferred to Mg^{++}-depleted medium at time zero. Bacteria were prepared for freeze-etching before transfer and at 3, 12, and 24 hr after transfer, as indicated by the arrows. An OD of 0.100 represented 4 × 10^7 to 5 × 10^7 bacteria per ml.*

cracked exponentially growing cells in the cell wall and in the plasma membrane (Fig. 3 to 5, 7). The outermost wall layer that broke off was about half the thickness of the following layer which comprised the rest of the wall and part or all of the cell membrane. The relative width of the outer layer suggests that the fracture may occur in the "soft layer" of de Petris (20), that is, at the outer triple-layered structure seen in thin-section micrographs.

Fractures along the convex face of the plasma membrane ($\widehat{M}$) exposed a netlike arrangement of particles 2 to 6 nm in diameter (Fig. 3 and 4), whereas the concave membrane face ($\breve{M}$; Fig. 3 and 5) showed only scattered particles of the same size. We could demonstrate that both $\widehat{M}$ and $\breve{M}$ are views of the plasma membrane (and not wall material) by examining plasmolyzed cells (not illustrated) in which the cell membrane was completely retracted from the cell wall. Apparent connections between the membrane and the overlying wall layers (Fig. 3a) may be real fibers or artifacts of the fracture process (6). They have been noted in other bacteria (23).


2

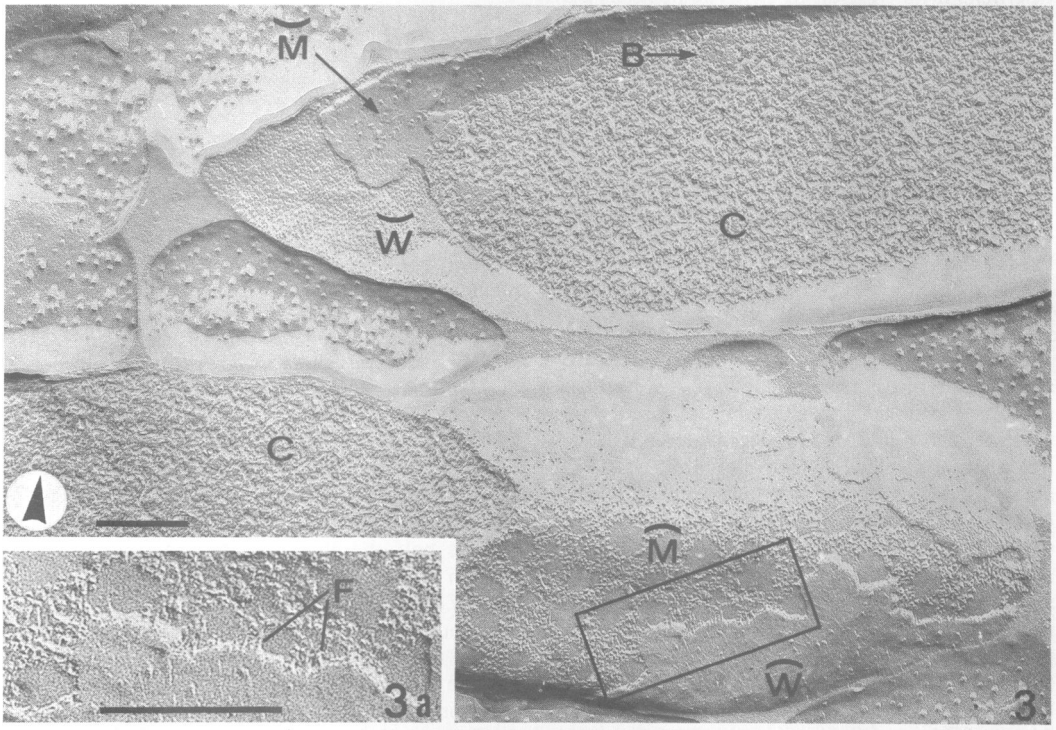
M
B
W
C
C
M
W
3

F
3a

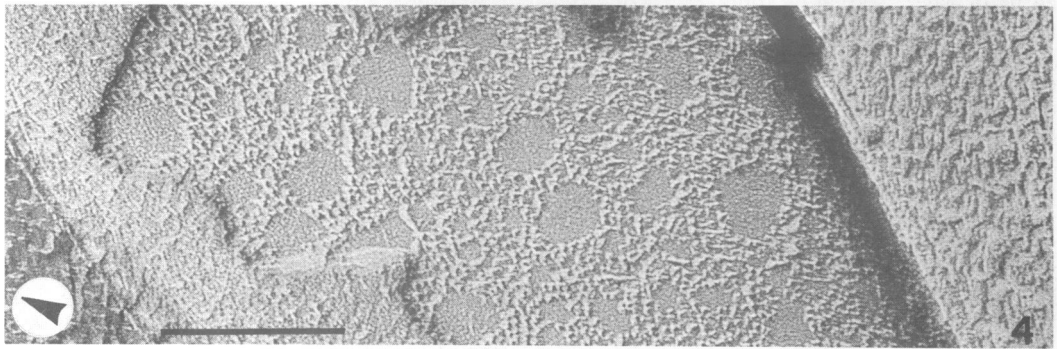
4

Fractures through the cell (Fig. 3 and 7) revealed two distinct features in the otherwise granular cytoplasm: small circular bodies, also observed in thin-section electron micrographs (9; Fiil, *unpublished data*), and internal membranes close to the poles of the bacteria. The latter were identical in structure to the plasma membrane, except for a reversal of the concave/convex faces (compare Fig. 5 and 6, Fig. 4 and 7). Thus, the internal membranes are most likely invaginations from the plasma membrane.

Mg^{++} starved cells. Within a few hours after transfer to Mg^{++}-deficient media, a paracrystalline particle pattern (R) appeared on the plasma membranes (Fig. 8). This pattern was first seen 3 hr after transfer to Mg^{++}-deficient conditions and covered increasingly larger areas with prolonged starvation (Fig. 10 and 12). Particle periodicity in the array was 6 by 6 nm. Within 12 hr after the removal of magnesium, two further changes of the membranes were conspicuous: infoldings (Fig. 9 and 12) and smooth areas devoid of particles (Fig. 11). The infolded membranes had the same appearance as the cytoplasmic membrane and showed the normal netlike pattern as well as the smooth and paracrystalline Mg^{++}-starved patterns. The widths of both the normal plasma membranes and the invaginated membranes seen during Mg^{++} starvation were 7 to 8 nm. After 24 hr in the Mg^{++}-deficient medium, the cells fractured only in the membranes and no longer in the wall. The same preferential split was seen in cells starved of calcium (*unpublished data*). However, the Ca^{++}-starved cells remained viable and the membranes appeared normal except for large areas devoid of particles.

Addition of magnesium to the culture after 12 hr, when 100% of the bacteria were still viable, did not reverse the particle pattern characteristic of Mg^{++} starvation for at least 4 hr, during which time the cell mass doubled. It appeared that the abnormal membranes were diluted out by growth.

Mg^{++} determinations. The paracrystalline pattern found during Mg^{++} starvation could have been due to a lowered concentration of Mg^{++} ions in either the entire cell or specifically the membrane. Although a homogeneous membrane fraction could not be isolated, the Mg^{++} content was determined in each of the two purified fractions containing both membrane and wall. The most interesting and unexpected result of these measurements was that, even though the total Mg^{++} content of starved cells was reduced two- to threefold, there was no significant difference at any time between the Mg^{++} concentration of cell envelopes of exponentially growing bacteria and Mg^{++}-starved bacteria. The Mg^{++} content of the envelopes was 40 to 45 μmoles of Mg^{++} per gram (dry weight) of walls.

DISCUSSION

E. coli has the potential to change the structure of its plasma membrane in response to alterations in the cell environment. These changes involve not only the proliferation and infolding of the cell membrane reported previously (9, 16) but also the rearrangement of particulate structures in the plane of the membrane. Although we do not yet have direct indications regarding the location of these units within the *E. coli* cell membrane, the available experimental evidence suggests that the preferred plane of fracture during freeze-etching occurs between hydrophobically bonded structures, such as exist within biological membranes (2, 3, 10). If this is also true for *E. coli* cells, it means that the membrane features illustrated in this report are those of an inner membrane face rather than of the membrane surface. Hence, the particles seen on the fracture faces would be embedded within the interior of the membrane matrix. However, if, for some reason, the *E. coli* cell membrane fractures differently from most other biological membranes, then the exposed faces could be the true membrane surface and the netlike and semicrystalline particle arrays would be on the membrane surface rather than in the membrane matrix. Although our work with *E. coli* does not distinguish clearly between these two possibilities, both imply that the development of paracrystalline particle arrays during growth in Mg^{++}-deficient media is intimately connected with structural rearrangements of the *E. coli* cell membrane.

The function and chemical composition of the particles seen in *E. coli* membranes, as well as in most other membranes revealed by freeze-etching, are unknown. Active membranes, e.g., those capable of photosynthetic activity (4, 11, 19), photoreception (6), or active transport (27), have many such particles, whereas inactive membranes,

FIG. 2. *Surface of exponentially growing E. coli B/r/1 seen after etching for 15 min at −98 C. No glycerol treatment was used in this preparation. Magnification markers in this and in the following figures represent 0.2 μm.*

FIG. 3. *Exponentially grown cells showing the cytoplasm (C) with a circular body (B), convex ($\widetilde{M}$) and concave ($\widetilde{M}$) plasma membrane faces, and two wall faces ($\widetilde{W}$ and $\widetilde{W}$). Figure 3a shows fiberlike connections (F) between the membrane and the wall.*

FIG. 4. *Convex plasma membrane face of an exponentially grown cell. A portion of the wall is visible on the left.*

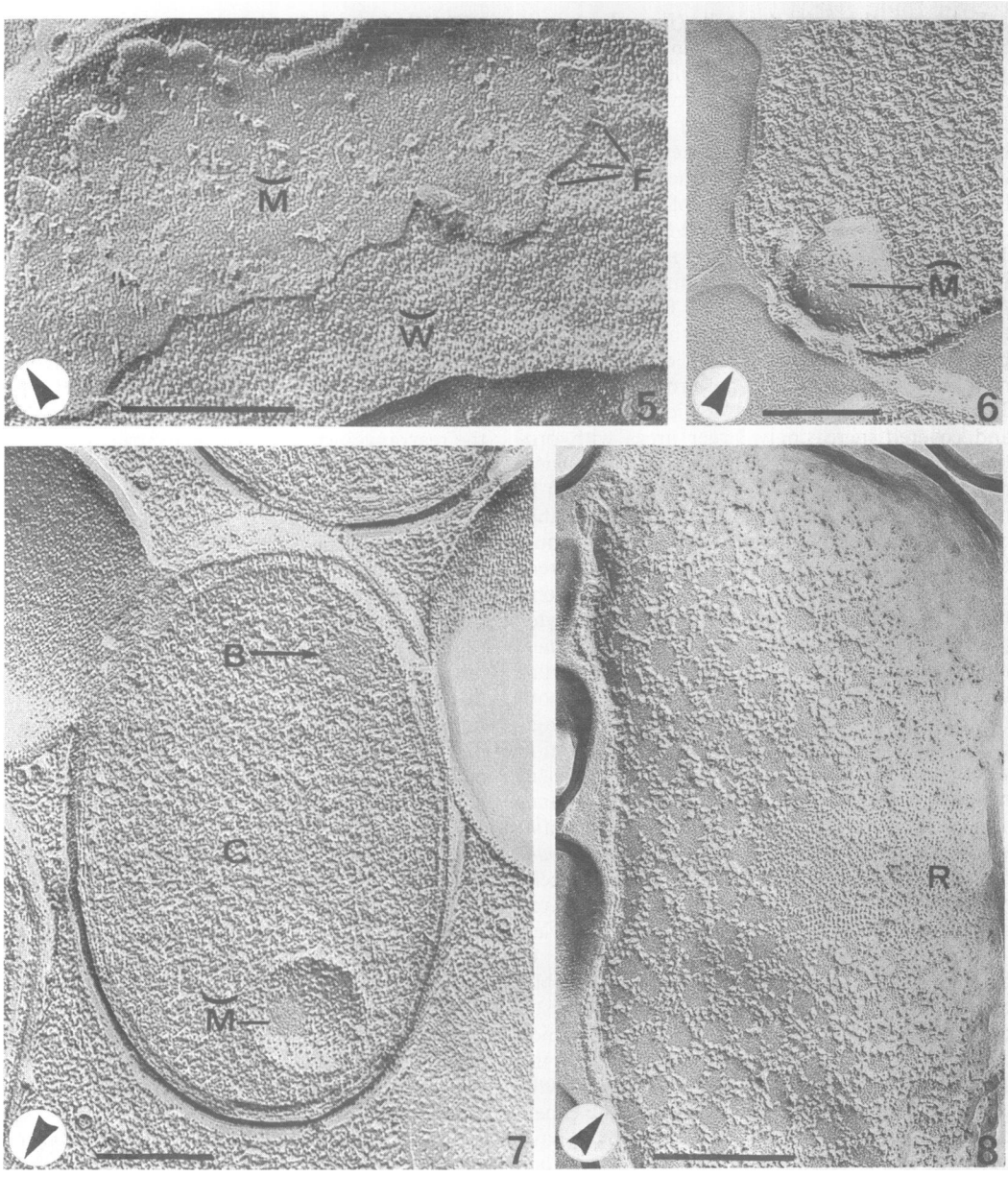

FIG. 5. *Exponentially grown cell. The concave faces of the plasma membrane ($\breve{M}$) and wall ($\breve{W}$) with fiberlike connections (F).*

FIG. 6. *Exponentially grown cell. Particle distribution on the convex internal membrane face ($\hat{M}$) is similar to the distribution on the concave plasma membrane face ($\breve{M}$, Fig. 5).*

FIG. 7. *Exponentially grown cell. Fracture through the cytoplasm (C) with circular body (B). Particle distribution on the concave internal membrane face ($\breve{M}$) is comparable to that on the convex plasma membrane face (Fig. 4).*

FIG. 8. *Convex plasma membrane face of E. coli after 12 hr of Mg^{++} starvation. A paracrystalline particle pattern (R) has appeared.*

e.g., insulating layers of myelin (3), are smooth and devoid of the particles. The particles may represent micellar transitions within an otherwise predominantly lamellar system (12, 13) or protein embedded in the membrane (15, 26). Furthermore, the freeze-etch image of the particles may reflect in vivo membrane structure or chemical domains that have a greater tendency than others

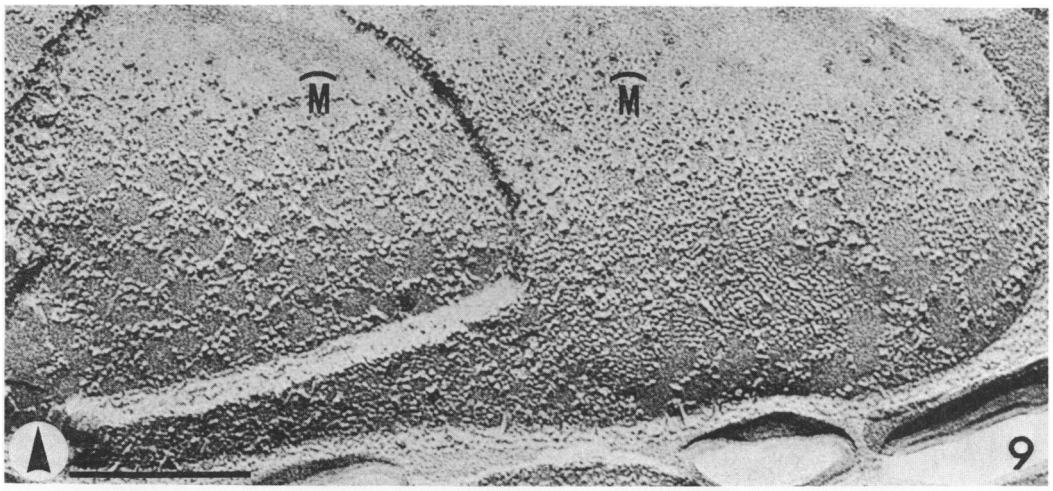

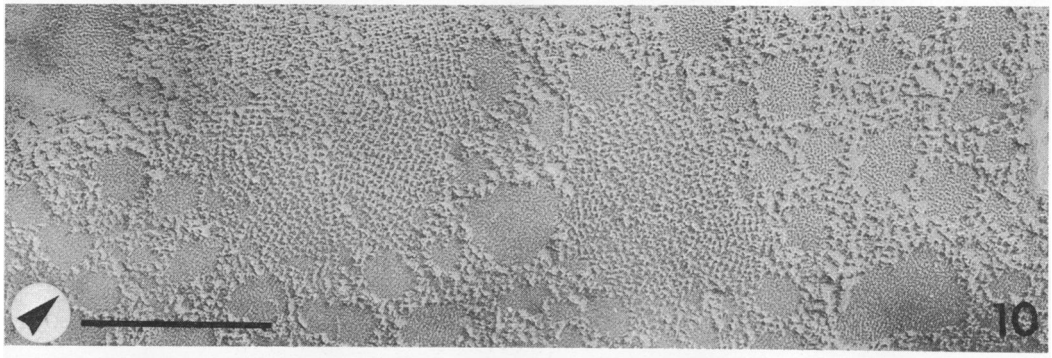

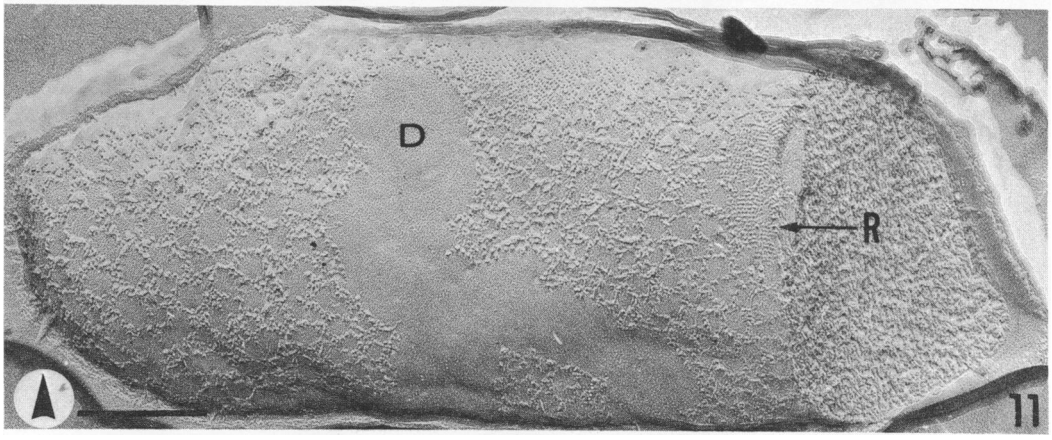

FIG. 9. *E. coli after 12 hr of Mg^{++} starvation. Invagination of the cell membrane builds up several membrane layers ($\hat{M}$) exposed by the fracture process.*

FIG. 10. *Convex plasma membrane face of E. coli after 24 hr of Mg^{++} starvation.*

FIG. 11. *E. coli starved of Mg^{++} for 24 hr. Large areas devoid of particles (D), as well as particle arrays (R), are seen on the plasma membrane.*

to deform during fracture (6). Again, although we do not yet have experimental evidence that distinguishes among these several possiblities, it is clear that the very regular and reproducible freeze-etch image must be substantially dependent upon the molecular ordering within the *E. coli* membranes.

Although molecular reordering in response to

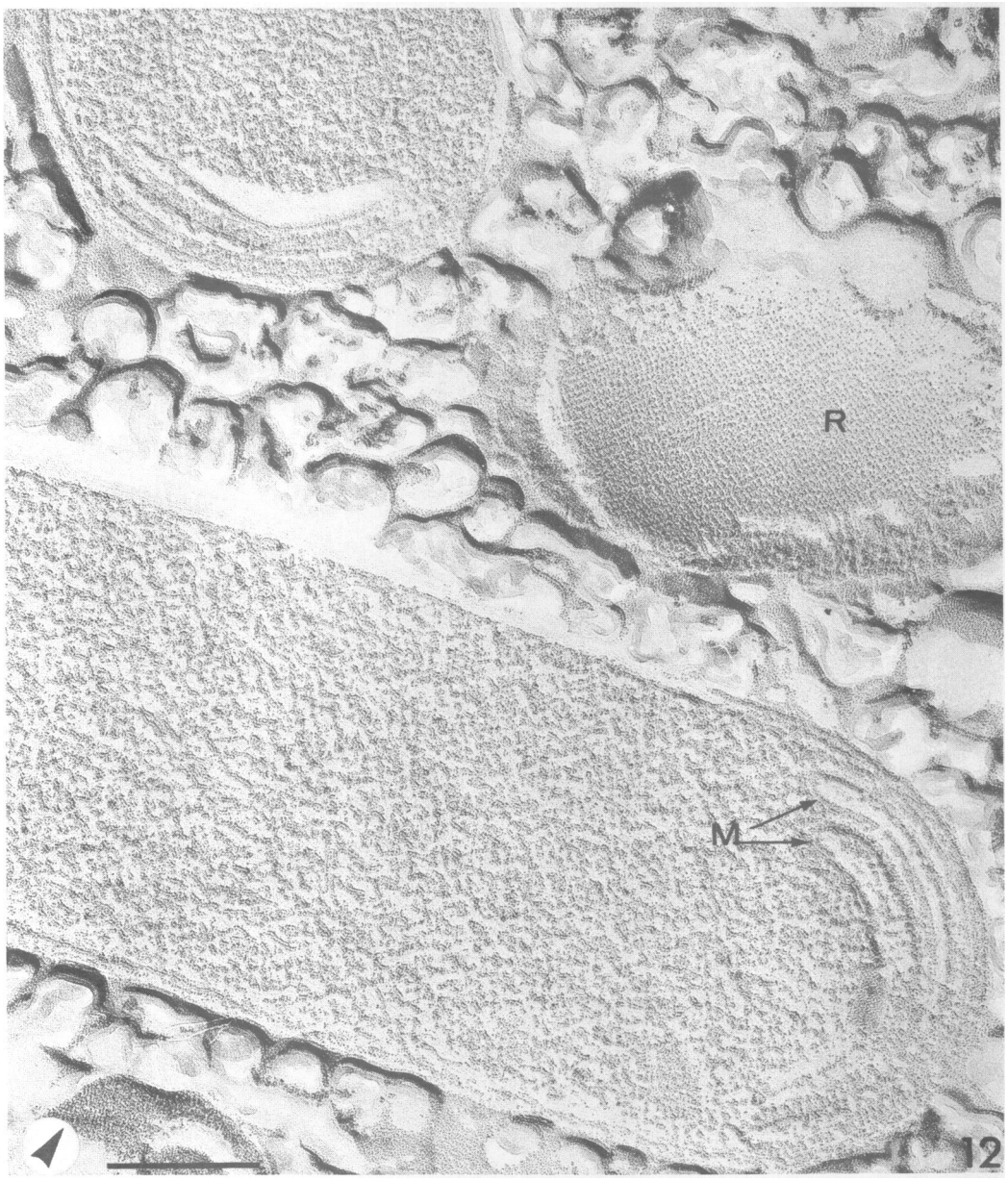

FIG. 12. *E. coli starved of Mg^{++} for 24 hr. The invaginated membranes (M) are seen in cross-fracture. The convex plasma membrane face of one cell is covered with arrayed particles (R).*

environment is often postulated to account for membrane-associated phenomena (20), there are few reports in which reordering of structure within a membrane has been observed by electron microscopy. With standard thin-sectioning techniques, Brandt and Freeman (1) noted rapid changes in amoeba membrane thickness which correlated with changes in electrical resistance. As with *E. coli*, alterations in membrane morphology were induced by changes in the environment of the cells, but in contrast to the changes noted in amoeba the alterations in *E. coli* appear to be slow and irreversible. We saw the first evidence of paracrystalline particle arrays 3 hr after transfer to Mg^{++}-depleted media. Furthermore, addition of Mg^{++} to the culture did not eliminate the paracrystalline pattern, although the cells did dilute out the arrays with normal growth. Thus,

the paracrystalline patterns seen in the cell membrane of *E. coli* appear to be a developmental modification induced by Mg^{++} starvation rather than the direct response of a normal membrane to a low Mg^{++} environment. This is consistent with the fact that Mg^{++} concentrations did not decrease in the cell envelope itself, suggesting that Mg^{++} deprivation affected membrane structure indirectly, via other perturbances in cell metabolism, e.g., ribosome breakdown (8, 14).

In *E. coli*, a general response to stress [Ca or C source deprivation (*unpublished data* as well as the Mg^{++} starvation experiments reported here)] is a derangement of the particles on the plasma membrane and the appearance of smooth areas, such as those illustrated in Fig. 11. However, the paracrystalline arrays neighboring on these smooth areas were never seen in Ca-starved or C source-starved cells. They appear to be uniquely associated with Mg^{++} starvation.

ACKNOWLEDGMENTS

We thank Donald A. Glaser for providing laboratory facilities for part of this work.

This research was supported by Atomic Energy Commission contract AT(11-1)-34, P. A. 142.

LITERATURE CITED

1. Brandt, P. W., and A. R. Freeman. 1967. Plasma membrane: substructural changes correlated with electrical resistance and pinocytosis. Science 155:582–585.
2. Branton, D. 1966. Fracture faces of frozen membranes. Proc. Nat. Acad. Sci. U.S.A. 55:1048–1056.
3. Branton, D. 1967. Fracture faces of frozen myelin. Exp. Cell Res. 45:703–707.
4. Branton, D., and R. B. Park. 1967. Subunits in chloroplast lamellae. J. Ultrastruct. Res. 19:283–303.
5. Brock, T. D. 1962. Effects of magnesium ion deficiency on *Escherichia coli* and possible relation to the mode of action of novobiocin. J. Bacteriol. 84:679–682.
6. Clark, A. W., and D. Branton. 1968. Fracture faces in frozen outer segments from the guinea pig retina. Z. Zellforsch. 91:586–603.
7. Clark, D. J., and O. Maaløe. 1967. DNA replication and the division cycle in *Escherichia coli*. J. Mol. Biol. 23:99–112.
8. Cohen, P. S., and H. L. Ennis. 1967. Amino acid regulation of RNA synthesis during recovery of *Escherichia coli* from magnesium starvation. Biochim. Biophys. Acta 145:300–309.
9. Cota-Robles, E. H. 1966. Internal membranes in cells of *Escherichia coli*. J. Ultrastruct. Res. 16:626–639.
10. Deamer, D. W., and D. Branton. 1967. Fracture planes in an ice-bilayer model membrane system. Science 158:655–657.
11. Giesbrecht, P., and G. Drews. 1966. Über die Organisation und die makromolekulare Architecture der Thylakoide "lebender" Bakterien. Arch. Mikrobiol. 54:297–330.
12. Kavanau, J. L. 1966. Membrane structure and function. Fed. Proc. 25:1096–1107.
13. Lucy, J. A. 1964. Globular lipid micelles and cell membranes. J. Theor. Biol. 7:360–373.
14. McCarthy, B. J. 1962. The effects of magnesium starvation on the ribosome content of *Escherichia coli*. Biochim. Biophys. Acta 55:880–888.
15. Mitchell, P. 1957. A general theory of membrane transport from studies of bacteria. Nature 180:134–136.
16. Morgan, C., H. S. Rosenkranz, B. Chan, and H. M. Rose. 1966. Electron microscopy of magnesium-depleted bacteria. J. Bacteriol. 91:891–895.
17. Moor, H., and K. Mühlethaler. 1963. Fine structure in frozen-etched yeast cells. J. Cell Biol. 17:609–628.
18. Moor, H., K. Mühlethaler, H. Waldner, and A. Frey-Wyssling. 1961. A new freezing-ultramicrotome. J. Biophys. Biochem. Cytol. 10:1–13.
19. Mühlethaler, K., H. Moor, and J. W. Szarkowski. 1965. The ultrastructure of the chloroplast lamellae. Planta 67:305–323.
20. Penniston, J. T., and D. E. Green. 1968. The conformational basis of energy transformations in membrane systems. IV. Energized states and pinocytosis in erythrocyte ghosts. Arch. Biochem. Biophys. 128:339–350.
21. de Petris, S. 1967. Ultrastructure of the cell wall of *Escherichia coli* and chemical nature of its constituent layers. J. Ultrastruct. Res. 19:45–83.
22. Remsen, C. C. 1968. Fine structure of the mesosome and nucleoid in frozen-etched *Bacillus subtilis*. Arch. Mikrobiol. 61:40–47.
23. Remsen, C., and D. G. Lundgren. 1966. Electron microscopy of the cell envelope of *Ferrobacillus ferrooxidans* prepared by freeze-etching and chemical fixation techniques. J. Bacteriol. 92:1765–1771.
24. Schleif, R. 1967. Control of ribosomal protein. J. Mol. Biol. 27:41–55.
25. Steere, R. L. 1957. Electron microscopy of structure detail in frozen biological specimens. J. Biophys. Biochem. Cytol. 3:45–60.
26. Wallach, D. F. H., and P. H. Zahler. 1966. Protein conformations in cellular membranes. Proc. Nat. Acad. Sci. U.S.A. 56:1552–1559.
27. Weinstein, R. S., and S. Bullivant. 1967. The application of freeze-cleaving technics to studies on red blood cell fine structure. Blood 29:780–789.